

Coverage Analysis of Hybrid RF/THz Networks With Best Relay Selection

Zhengying Lou, Baha Eddine Youcef Belmekki, and Mohamed-Slim Alouini, *Fellow, IEEE*

Abstract—Utilizing terahertz (THz) transmission to enhance coverage has proven various benefits compared to traditional radio frequency (RF) counterparts. This letter proposes a dual-hop decode-and-forward (DF) routing protocol in a hybrid RF and THz relay network named hybrid relay selection (HRS). The coverage probability of the HRS protocol is derived. The HRS protocol prioritizes THz relays for higher data rates or short source-destination distances; and RF relays for lower data rates or large source-destination distances. The proposed HRS protocol offers nearly the same performance as the optimal selection protocol, which requires complete instantaneous channel state information (CSI) of all the nodes.

Index Terms—Stochastic geometry, hybrid RF and THz relay network, relay selection, coverage probability.

I. INTRODUCTION

With the upcoming bandwidth-hungry applications of the sixth generation (6G) networks such as virtual reality (VR) and holographic communications, ubiquitous and ultra-high-speed access are required [1]. Utilizing the terahertz (THz) band will increase channel bandwidth and transmission capacity as it is considered one of the key enablers of 6G networks [2]. Compared to traditional radio frequency (RF) networks, dense THz networks have lower power consumption, smaller time delay, weaker radiation, better beam directivity, and higher interference immunity [3]. However, THz signals suffer from deep fading due to large free space path-loss and water molecule absorption, which significantly limit the effective communication distance [4]. Hence, relay communications are used to cope with this limitation.

Most of the literature focuses on coverage performance for a given relay link [5]–[7]. The works in [5], [6] studied the outage probability, which is the complementary cumulative distribution function of the coverage probability, of dual-hop THz-THz links, and [6] further optimized the transmission power. In [7], the authors derived the outage probability and the ergodic capacity of dual-hop THz-RF links, respectively. However, the above distance-fixed three-point (source-relay-destination) model is simplified for a dense DF THz network. The authors in [8] analyzed the downlink coverage probability of the hybrid RF and THz network, but relay communication is not considered.

Against this background, THz relay selection strategies are lacking in the literature. Moreover, since THz base stations are expected to coexist with RF base stations, a relay selection mechanism involving both THz and RF relays is necessary especially for ultra-dense networks (UDNs) and integrated access and backhaul (IAB) deployments. In this treatise, we propose a hybrid relay selection (HRS) protocol with RF

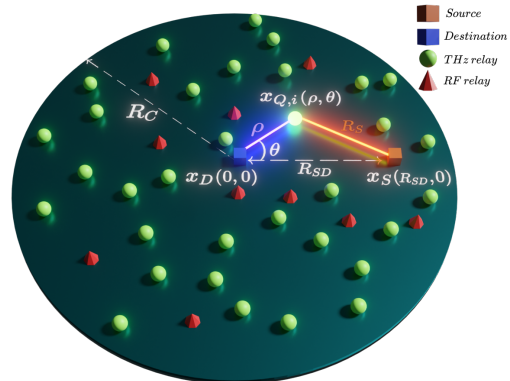


Fig. 1: System model.

and THz relays. Furthermore, the mathematical derivations are based on a realistic THz channel model that follows $\alpha - \mu$ which is an experimentally validated model [9], and the relays are randomly located following a Poisson point process (PPP). The aim of this letter is to investigate the performance of the proposed protocol and how the relay selection is carried out when both RF and THz relays are involved in the selection process. Our proposed HRS protocol is compared with the optimal relay selection that requires a full and perfect instantaneous channel state information (CSI) of all nodes in the networks which is impractical to estimate. We also show when to use RF relays and/or THz relays. Finally, for the sake of completeness, we compare our protocol with RF and THz direct transmissions.

II. SYSTEM MODEL

A. Network Model

We consider the system model depicted in Fig. 1. Without loss of generality, we set the position of a destination (D) at the origin for tractability since the same performance is obtained for any other D locations due to Slivnyak's Theorem. Also, the direction from a source (S) to D is the positive x -axis. In polar coordinate (ρ, θ) , the positions of S and D can be denoted as $x_S(R_{SD}, 0)$ and $x_D(0, 0)$, respectively, where R_{SD} is the distance between S and D . The locations of Q relays form a homogeneous PPP denoted by $\Phi_Q = \{x_{Q,1}, x_{Q,2}, \dots\}$ and with density λ_Q , where Q is replaced by RF in RF networks, and by THz in THz networks. We assume Φ_{RF} and Φ_{THz} are independent. All RF and THz relays, referred to as all nodes, are located on a two-dimensional circular disc $\mathcal{C}(x_D, R_C)$ centered at the origin with radius R_C . Note that the relays outside $\mathcal{C}(x_D, R_C)$ are not considered since they are far from D and suffer a large signal attenuation. Hence, $\mathcal{C}(x_D, R_C)$ is equivalent to the entire \mathbb{R}^2 . We assume that the locations of S , D , and the relays and the frequency band of the relays are shared, so the beams have been trained, and the communication targets are always within the main lobe of beams. Owing to the utilization of orthogonal sub-bands and

The authors are with King Abdullah University of Science and Technology (KAUST), CEMSE division, Thuwal 23955-6900, Saudi Arabia (e-mail: zhengying.lou@kaust.edu.sa; bahaeddine.belmekki@kaust.edu.sa; slim.alouini@kaust.edu.sa).

narrow-beam transmission, it is extremely uncommon that the interference signal in the same sub-band is placed in the main lobe of the receiving device, hence the interference is minor compared to noise.

B. Channel Model

1) *RF Channel Model*: RF channels experience path-loss and small-scale fading; therefore, the corresponding received power can be expressed as, $h_{\text{RF}}(R_X) = \varepsilon_{\text{RF}} G_{\text{RF}} \gamma_{\text{RF}} R_X^{-\beta_{\text{RF}}} \mathcal{X}_{\text{RF}}$, where $X = \{S, D\}$, R_X is the distance between a relay and X , ε_{RF} is the transmitting power, and G_{RF} is total antenna gain. The path-loss is modeled as $\gamma_{\text{RF}} R_X^{-\beta_{\text{RF}}}$, where β_{RF} is the path-loss exponent, $\gamma_{\text{RF}} = (c/4\pi\nu_{\text{RF}})^2$, $c = 3 \times 10^8$ m/s is the speed of light, and ν_{RF} is the RF carrier frequency. The small-scale fading \mathcal{X}_{RF} is subject to an exponential distribution with unit mean. The signal-to-noise ratio (SNR) of the RF channel is given by

$$\text{SNR}_{\text{RF},X} = \frac{\varepsilon_{\text{RF}} G_{\text{RF}} \gamma_{\text{RF}} R_X^{-\beta_{\text{RF}}} \mathcal{X}_{\text{RF}}}{\sigma_{\text{RF}}^2}, \quad (1)$$

where σ_{RF}^2 is the thermal noise. We note that σ_{RF}^2 is a function of the transmission bandwidth B_{RF} .

2) *THz Channel Model*: According to [8], the received power in THz transmission is modeled as, $h_{\text{THz}}(R_X) = \varepsilon_{\text{THz}} G_{\text{THz}} \gamma_{\text{THz}} \mathcal{X}_{\text{THz}} \exp(-\beta_{\text{THz}} R_X)/R_X^2$, where $X = \{S, D\}$, R_X is the distance between a relay and X , ε_{THz} is the transmitting power, and G_{THz} is the total antenna gain. The path-loss is modeled as $\gamma_{\text{THz}} \exp(-\beta_{\text{THz}} R_X)/R_X^2$, where $\gamma_{\text{THz}} = (c/4\pi\nu_{\text{THz}})^2$, ν_{THz} is the THz carrier frequency in GHz, and β_{THz} is the molecular absorption coefficient related to ν_{THz} . The small-scale fading \mathcal{X}_{THz} is modeled as $\alpha - \mu$ distribution which is an experimentally validated fading model for THz frequencies [9]. Moreover, α denotes the fading parameter and μ denotes the normalized variance of the channel fading. The complementary cumulative distribution function (CCDF) of \mathcal{X}_{THz} is given by $\bar{F}_{\mathcal{X}_{\text{THz}}}(m) = \Gamma(\mu, \mu m^{\frac{\alpha}{2}})/\Gamma(\mu)$, where $\Gamma(\mu, \mu m^{\frac{\alpha}{2}})$ and $\Gamma(\mu)$ are the upper incomplete Gamma function and the Gamma function, respectively [10]. The SNR of the THz channel is given by

$$\text{SNR}_{\text{THz},X} = \frac{\varepsilon_{\text{THz}} G_{\text{THz}} \gamma_{\text{THz}} \exp(-\beta_{\text{THz}} R_X) \mathcal{X}_{\text{THz}}}{\sigma_{\text{THz}}^2 R_X^2}, \quad (2)$$

where σ_{THz}^2 is the thermal noise, which is a function of the transmission bandwidth B_{THz} .

C. Relay Selection Strategy

Due to excessive path-loss and blockage, a half-duplex DF relay protocol is adopted since the direct link may be blocked. In fixed topology DF networks, the optimal relay selection relies on the maximization of end-to-end $\text{SNR}_{Q,X}$ or the maximization of the minimum $\text{SNR}_{Q,X}$ of $S - x_{Q,i}$ and $x_{Q,i} - D$ links. However, this protocol requires a full and perfect instantaneous CSI of all the nodes in the networks, that is, CSI between S and all relays, and between all relays and D . In addition, due to the randomness of the relay locations, analysis is intractable [11]. Therefore, we proposed a slightly suboptimal protocol that only requires instantaneous

CSI between S and all nodes while still being mathematically tractable. The protocol has the following selection strategy: we first select two sets of relays $\tilde{\Phi}_Q$ that can meet the attempted rate y_{th} of S . Among these sets, only the relay $x_{\text{RF},i} \in \tilde{\Phi}_{\text{RF}}$ or $x_{\text{THz},i} \in \tilde{\Phi}_{\text{THz}}$ that has the best link to D , that is, provides the maximum average rate with D is selected [8]. The set of relays that can establish reliable communication with S can be expressed as

$$\tilde{\Phi}_Q = \{x_{Q,i} \in \Phi_Q, \text{SNR}_{Q,S} \geq \tau_Q\}, \quad Q = \{\text{RF}, \text{THz}\}, \quad (3)$$

where τ_Q is a predefined threshold, $\text{SNR}_{Q,S}$ is the SNR of S -relay link. Subsequently, the relation between achievable rate $y_{Q,X}$ and $\text{SNR}_{Q,X}$ is given by

$$y_{Q,X} = \frac{B_Q}{2} \log_2(1 + \text{SNR}_{Q,X}), \quad (4)$$

where B_Q is the transmission bandwidth of Q link and the factor 1/2 is used because two time slots are required to transmit data via the relay node. The rate coverage probability is defined as the probability of achieving the desired rate y_{th} , i.e., $\text{SNR}_{Q,X} > \tau_Q = 2^{(2y_{th}/B_Q)} - 1$.

III. COVERAGE PROBABILITY OF HRS PROTOCOL

In this section, we derive the coverage probability, the intermediate distance distributions, and the association probabilities of the HRS protocol. Note that the nearest relay provides the largest average rate for D in our model, so the distance distributions are given in Lemmas.

Lemma 1. *The complementary cumulative distribution function (CCDF) of the distance between D and its nearest RF relay is given by*

$$\begin{aligned} \bar{F}_{R_D, \text{RF}}(r) = & \exp\left(-\int_0^r \int_0^{2\pi} \lambda_{\text{RF}} \exp\left(-\tau_{\text{RF}} \varepsilon_{\text{RF}}^{-1}\right.\right. \\ & \left.\left. \times \gamma_{\text{RF}}^{-1} (\rho^2 + R_{SD}^2 - 2\rho R_{SD} \cos\theta)^{\frac{\beta_{\text{RF}}}{2}} \sigma_{\text{RF}}^2\right) \rho \, d\theta d\rho.\right) \end{aligned} \quad (5)$$

where $0 < r \leq R_C$.

Then, the probability density functions (PDF) of the distance between D and its nearest RF relay is given by,

$$\begin{aligned} f_{R_D, \text{RF}}(r) = & r \lambda_{\text{RF}} \int_0^{2\pi} \exp\left(-\tau_{\text{RF}} \varepsilon_{\text{RF}}^{-1} G_{\text{RF}}^{-1} \gamma_{\text{RF}}^{-1}\right. \\ & \left. \times (\rho^2 + R_{SD}^2 - 2\rho R_{SD} \cos\theta)^{\frac{\beta_{\text{RF}}}{2}} \sigma_{\text{RF}}^2\right) d\theta \\ & \times \exp\left(-\int_0^r \int_0^{2\pi} \lambda_{\text{RF}} \exp\left(-\tau_{\text{RF}} \varepsilon_{\text{RF}}^{-1} G_{\text{RF}}^{-1} \gamma_{\text{RF}}^{-1}\right.\right. \\ & \left.\left. \times (\rho^2 + R_{SD}^2 - 2\rho R_{SD} \cos\theta)^{\frac{\beta_{\text{RF}}}{2}} \sigma_{\text{RF}}^2\right) \rho \, d\theta d\rho.\right) \end{aligned} \quad (6)$$

Proof. The CCDF of the distance can be derived by using the void probability of a homogeneous PPP [12]

$$\bar{F}_{R_D, \text{RF}}(r) = \mathbb{P}[\text{No relays in } \mathcal{C}(x_D, r)] = \exp(-\Lambda_{\text{RF}}(r)), \quad (7)$$

where $\mathcal{C}(x_D, r)$ is the disk centered at the origin (x_D) with radius r . The mean number of RF relays $x_{\text{RF},i} \in \Phi_{\text{RF}}$ in the circular disc $\mathcal{C}(x_D, r)$, denoted by $\Lambda_{\text{RF}}(r)$, can be written as

$$\Lambda_{\text{RF}}(r) = \int_0^r \int_0^{2\pi} \hat{\lambda}_{\text{RF}}(\rho, \theta) \rho d\theta d\rho, \quad (8)$$

where ρ and θ are the radial distance and polar angle in the polar coordinate system respectively, and $\hat{\lambda}_{\text{RF}}(\rho, \theta)$ is the density of $\tilde{\Phi}_{\text{RF}}$. The set $\tilde{\Phi}_{\text{RF}}$ can be regarded as a dependent-thinning of Φ_{RF} , and only the relays that have an $\text{SNR}_{\text{RF},S}$ greater than the threshold τ_{RF} are retained. Hence, the set $\tilde{\Phi}_{\text{RF}}$ is a inhomogeneous PPP of density $\hat{\lambda}_{\text{RF}}(\rho, \theta)$. The density $\hat{\lambda}_{\text{RF}}(\rho, \theta)$ can be derived as follows

$$\begin{aligned} \hat{\lambda}_{\text{RF}}(\rho, \theta) &= \lambda_{\text{RF}} \mathbb{P} \left[\frac{\varepsilon_{\text{RF}} G_{\text{RF}} \gamma_{\text{RF}} R_S^{-\beta_{\text{RF}}} \mathcal{X}_{\text{RF}}}{\sigma_{\text{RF}}^2} > \tau_{\text{RF}} \right] \\ &= \lambda_{\text{RF}} \mathbb{P} \left[\mathcal{X}_{\text{RF}} > \tau_{\text{RF}} \varepsilon_{\text{RF}}^{-1} G_{\text{RF}}^{-1} \gamma_{\text{RF}}^{-1} R_S^{\beta_{\text{RF}}} \sigma_{\text{RF}}^2 \right] \\ &= \lambda_{\text{RF}} \exp \left(-\tau_{\text{RF}} \varepsilon_{\text{RF}}^{-1} G_{\text{RF}}^{-1} \gamma_{\text{RF}}^{-1} R_S^{\beta_{\text{RF}}} \sigma_{\text{RF}}^2 \right), \end{aligned} \quad (9)$$

where R_S is the distance between S and relay and can be expressed as

$$R_S^2 = \rho^2 + R_{SD}^2 - 2\rho R_{SD} \cos \theta. \quad (10)$$

By substituting (8), (9), and (10) into (7), we obtain (5). Then, using $f_{R_D, \text{RF}}(r) = -\frac{d}{dr} \bar{F}_{R_D, \text{RF}}(r)$ and Leibniz integral rule, (6) is derived straightforwardly. \square

Lemma 2. *The CCDF and PDF of the distance between D and its nearest THz relay are given by (11) and (12), respectively, shown at the top of the next page.*

Proof. Following the same steps as in Lemma 1, we obtain

$$\bar{F}_{R_D, \text{THz}}(r) = \exp \left(-\int_0^r \int_0^{2\pi} \hat{\lambda}_{\text{THz}}(\rho, \theta) \rho d\theta d\rho \right), \quad (13)$$

where $\hat{\lambda}_{\text{THz}}(\rho, \theta)$ is the density of $\tilde{\Phi}_{\text{THz}}$, which is given by

$$\begin{aligned} \hat{\lambda}_{\text{THz}}(\rho, \theta) &= \lambda_{\text{THz}} \mathbb{P} \left[\frac{\varepsilon_{\text{THz}} G_{\text{THz}} \gamma_{\text{THz}} \mathcal{X}_{\text{THz}}}{\sigma_{\text{THz}}^2 \exp(\beta_{\text{THz}} R_S) R_S^2} > \tau_{\text{THz}} \right] \\ &= \lambda_{\text{THz}} \mathbb{P} \left[\mathcal{X}_{\text{THz}} > \frac{\tau_{\text{THz}} R_S^2 \exp(\beta_{\text{THz}} R_S) \sigma_{\text{THz}}^2}{\varepsilon_{\text{THz}} G_{\text{THz}} \gamma_{\text{THz}}} \right] \\ &\stackrel{(a)}{=} \frac{\lambda_{\text{THz}}}{\Gamma(\mu)} \Gamma \left(\mu, \mu \left(\frac{\tau_{\text{THz}} R_S^2 \exp(\beta_{\text{THz}} R_S) \sigma_{\text{THz}}^2}{\varepsilon_{\text{THz}} G_{\text{THz}} \gamma_{\text{THz}}} \right)^{\frac{\alpha}{2}} \right), \end{aligned} \quad (14)$$

where (a) follows the definition of the CCDF of \mathcal{X}_{THz} . Substituting (14) and (10) into (13) concludes the proof of (11). Similar to the proof of (6) in Lemma 1, (11) is given by $f_{R_D, \text{THz}}(r) = -\frac{d}{dr} \bar{F}_{R_D, \text{THz}}(r)$. \square

Using the above Lemmas, we derive the distribution of RF and THz relays that are closest to D . However, for the nearest RF relay to be selected, it is necessary to ensure that the achievable rate of THz transmission is less than that of RF transmission, and vice versa. Therefore, we calculate the (**selection**) association probabilities in the following two Lemmas.

Lemma 3. *Given that the distance between D and its nearest RF relay is r , the probability that D selects/associates with this RF relay is given by*

$$P_{\text{RF}}^A(r) = 1 - \int_0^{R_{\text{R2T}}(r)} f_{R_D, \text{THz}}(\rho) d\rho, \quad (15)$$

where R_{R2T} is given by

$$\begin{aligned} R_{\text{R2T}}(r) &= \frac{2}{\beta_{\text{THz}}} \times \\ &\mathcal{W} \left(\frac{\beta_{\text{THz}}}{2} \left(\left(1 + \frac{\varepsilon_{\text{RF}} G_{\text{RF}} \gamma_{\text{RF}}}{r^{\beta_{\text{RF}}} \sigma_{\text{RF}}^2} \right)^{\frac{\beta_{\text{RF}}}{\beta_{\text{THz}}}} - 1 \right) \frac{\sigma_{\text{THz}}^2}{\varepsilon_{\text{THz}} G_{\text{THz}} \gamma_{\text{THz}}} \right)^{-\frac{1}{2}}. \end{aligned} \quad (16)$$

We note that $\mathcal{W}(\cdot)$ is the Lambert \mathcal{W} -function defined as the inverse of the function $f_{\mathcal{W}}(m) = me^m$.

Proof. The distance of the nearest THz relay, denoted by R_{R2T} , can be solved by setting the average achievable rate of the RF relay with distance r to D equals to that of the THz relay with distance R_{R2T} to D [13]

$$\begin{aligned} \mathbb{E}_{\mathcal{X}_{\text{RF}}} [\text{SNR}_{\text{RF},D} | R_{\text{RF},D} = r] \\ = \mathbb{E}_{\mathcal{X}_{\text{THz}}} [\text{SNR}_{\text{THz},D} | R_{\text{THz},D} = R_{\text{R2T}}]. \end{aligned} \quad (17)$$

From the above equation, the relationship between R_{R2T} and r is given by (16). By the definition of association probability $P_{\text{RF}}^A(r)$ in Lemma 3 and the maximum average received power associated strategy, the following result is given

$$\begin{aligned} P_{\text{RF}}^A(r) &= \mathbb{P} [\text{No relays in } \mathcal{C}(x_D, R_{\text{R2T}})] = \\ &= 1 - \int_0^{R_{\text{R2T}}(r)} f_{R_D, \text{THz}}(\rho) d\rho. \end{aligned} \quad (18)$$

This concludes the proof of Lemma 3. \square

Lemma 4. *Given that the distance between D and its nearest THz relay is r , the probability that D selects/associates with this THz relay is given by*

$$P_{\text{THz}}^A(r) = 1 - \int_0^{R_{\text{T2R}}(r)} f_{R_D, \text{RF}}(\rho) d\rho, \quad (19)$$

where $f_{R_D, \text{RF}}(r)$ is defined in (6) and $R_{\text{T2R}}(r)$ is given by

$$\begin{aligned} R_{\text{T2R}}(r) = \\ \left(\left(1 + \frac{\varepsilon_{\text{THz}} G_{\text{THz}} \gamma_{\text{THz}}}{r^2 \exp(\beta_{\text{THz}} r) \sigma_{\text{THz}}^2} \right)^{\frac{\beta_{\text{THz}}}{\beta_{\text{RF}}}} - 1 \right) \frac{\sigma_{\text{RF}}^2}{\varepsilon_{\text{RF}} G_{\text{RF}} \gamma_{\text{RF}}} \right)^{-\frac{1}{\beta_{\text{RF}}}}. \end{aligned} \quad (20)$$

Proof. The proof of Lemma 4 is similar to that of Lemma 3 and therefore, omitted here. \square

Based on the distance distributions and association probabilities, the main result of this letter is given by the following theorem.

Theorem 1. *The coverage probability at D using the HRS protocol is given by*

$$\begin{aligned} P^C &= \int_0^{R^C} f_{R_D, \text{RF}}(\rho) \exp \left(-\frac{\tau_{\text{RF}} \rho^{\beta_{\text{RF}}} \sigma_{\text{RF}}^2}{\varepsilon_{\text{RF}} G_{\text{RF}} \gamma_{\text{RF}}} \right) P_{\text{RF}}^A(\rho) d\rho \\ &+ \int_0^{R^C} f_{R_D, \text{THz}}(\rho) P_{\text{THz}}^A(\rho) \frac{1}{\Gamma(\mu)} \\ &\times \Gamma \left(\mu, \mu \left(\frac{\tau_{\text{THz}} \rho^2 \sigma_{\text{THz}}^2}{\varepsilon_{\text{THz}} G_{\text{THz}} \gamma_{\text{THz}} \exp(-\beta_{\text{THz}} \rho)} \right)^{\frac{\alpha}{2}} \right) d\rho. \end{aligned} \quad (21)$$

$$\bar{F}_{R_D, \text{THz}}(r) = \exp \left(-\frac{\lambda_{\text{THz}}}{\Gamma(\mu)} \int_0^r \int_0^{2\pi} \Gamma \left(\mu, \mu \left(\frac{\tau_{\text{THz}} (\rho^2 + R_{SD}^2 - 2\rho R_{SD} \cos \theta) \sigma_{\text{THz}}^2}{\varepsilon_{\text{THz}} G_{\text{THz}} \gamma_{\text{THz}} \exp \left(-\beta_{\text{THz}} (\rho^2 + R_{SD}^2 - 2\rho R_{SD} \cos \theta)^{\frac{1}{2}} \right)} \right)^{\frac{\alpha}{2}} \right) \rho d\theta d\rho \right). \quad (11)$$

$$f_{R_D, \text{THz}}(r) = r \frac{\lambda_{\text{THz}}}{\Gamma(\mu)} \int_0^{2\pi} \Gamma \left(\mu, \mu \left(\frac{\tau_{\text{THz}} (r^2 + R_{SD}^2 - 2r R_{SD} \cos \theta) \sigma_{\text{THz}}^2}{\varepsilon_{\text{THz}} G_{\text{THz}} \gamma_{\text{THz}} \exp \left(-\beta_{\text{THz}} (r^2 + R_{SD}^2 - 2r R_{SD} \cos \theta)^{\frac{1}{2}} \right)} \right)^{\frac{\alpha}{2}} \right) d\theta \quad (12)$$

$$\times \exp \left(-\frac{\lambda_{\text{THz}}}{\Gamma(\mu)} \int_0^r \int_0^{2\pi} \Gamma \left(\mu, \mu \left(\frac{\tau_{\text{THz}} (\rho^2 + R_{SD}^2 - 2\rho R_{SD} \cos \theta) \sigma_{\text{THz}}^2}{\varepsilon_{\text{THz}} G_{\text{THz}} \gamma_{\text{THz}} \exp \left(-\beta_{\text{THz}} (\rho^2 + R_{SD}^2 - 2\rho R_{SD} \cos \theta)^{\frac{1}{2}} \right)} \right)^{\frac{\alpha}{2}} \right) \rho d\theta d\rho \right).$$

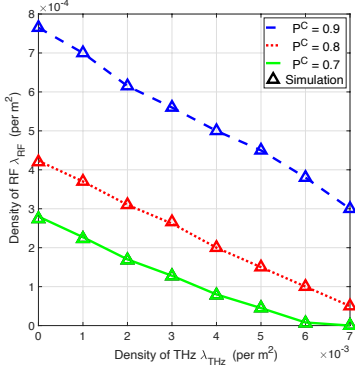


Fig. 2: Density of RF and THz relays under the same coverage probability of HRS.

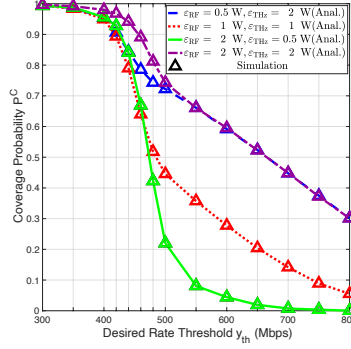


Fig. 3: Impact of transmission power and desired rate threshold on HRS.

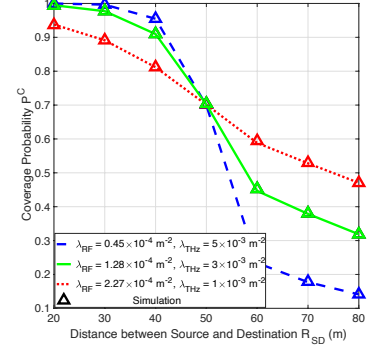


Fig. 4: Impact of relay density and source-destination distance on HRS.

Proof. The coverage probability P^C is defined as the probability that the received $\text{SNR}_{Q,D}$ at the receiver D from the selected Q relay is above the predefined threshold τ_Q , i.e., $P^C = \mathbb{P}[\text{SNR}_{Q,D} > \tau_Q]$. We divide the overall coverage probability P^C into coverage probability associated with RF relay P_{RF}^C and coverage probability associated with THz relay P_{THz}^C , i.e., $P^C = P_{\text{RF}}^C + P_{\text{THz}}^C$. Furthermore, P_{RF}^C can be obtained by (i) solving the coverage probability given that the distance of $S - x_{\text{RF},i}$ is $R_{\text{RF},D} = \rho$; (ii) multiplying the coverage probability with the association probability given that the distance of $S - x_{\text{RF},i}$ is $R_{\text{RF},D} = \rho$ (which is denoted as $P_{\text{RF}}^A(\rho)$); (iii) compute the expectation \mathbb{E}_ρ . Hence, P_{RF}^C is calculated as follows

$$\begin{aligned} P_{\text{RF}}^C &= \mathbb{E}_\rho \left[\mathbb{P}[\text{SNR}_{\text{RF},D} > \tau_{\text{RF}} | R_{\text{RF},D} = \rho] P_{\text{RF}}^A(\rho) \right] \\ &= \mathbb{E}_\rho \left[\exp \left(-\frac{\tau_{\text{RF}} \rho^{\beta_{\text{RF}}} \sigma_{\text{RF}}^2}{\varepsilon_{\text{RF}} G_{\text{RF}} \gamma_{\text{RF}}} \right) P_{\text{RF}}^A(\rho) \right] \\ &= \int_0^{R_C} f_{R_D, \text{RF}}(\rho) \exp \left(-\frac{\tau_{\text{RF}} \rho^{\beta_{\text{RF}}} \sigma_{\text{RF}}^2}{\varepsilon_{\text{RF}} G_{\text{RF}} \gamma_{\text{RF}}} \right) P_{\text{RF}}^A(\rho) d\rho. \end{aligned} \quad (22)$$

The proof of P_{THz}^C is similar to the proof of P_{RF}^C , therefore, it is omitted here. We note that the association probability P_Q^A is contained in the coverage probability associated with Q relay P_Q^C . By using $P^C = P_{\text{RF}}^C + P_{\text{THz}}^C$, the overall coverage probability is derived. \square

IV. NUMERICAL RESULTS

In this section, we provide selected simulation results to demonstrate the performance of the proposed HRS protocol. The simulations coincide perfectly with the theoretical analysis, and each simulation is performed over 10^6 independent network realizations within a circular disc of radius $R_C = 200$ m. We consider the THz link with an antenna gain

$G_{\text{THz}} = 40$ dBi and a carrier frequency $\nu_{\text{THz}} = 1.8$ THz. The corresponding absorption value β_{THz} is chosen from the realistic database, which is 0.2 m^{-1} [14]. To simulate the $\alpha - \mu$ channel, we set $\alpha = 2$ and $\mu = 4$ for the THz link. The carrier frequency ν_{RF} of the RF link is 2.1 GHz. The antenna gain G_{RF} is 20 dBi and path-loss exponent $\beta_{\text{RF}} = 2.5$. We set the noise power to -174 dBm/Hz for both links such as $\sigma_Q^2 = -174 + 10 \log_{10} B_Q$ dBm, while the transmission bandwidths $B_{\text{RF}} = 40$ MHz and $B_{\text{THz}} = 0.5$ GHz, by calculation $\sigma_{\text{RF}}^2 = -98$ dBm and $\sigma_{\text{THz}}^2 = -87$ dBm.

Fig. 2 shows the density of RF and THz relays in the HRS protocol required to achieve a given coverage probability when $\varepsilon_Q = 1$ W, $R_{SD} = 50$ m, and $y_{th} = 420$ Mbps. For a given coverage probability, when λ_{THz} increases linearly, λ_{RF} decreases roughly linearly. Moreover, when the coverage probability grows from 0.7 to 0.9, the slopes of the three curves increase consecutively, but the amplitude of the increase is quite small. Specifically, approximately 20 additional THz relays are required for 1 RF relay reduced to maintain the same coverage probability for an area of $2 \times 10^4 \text{ m}^2$.

In Fig. 3, we keep $R_{SD} = 50$ m and select a set of densities with coverage of 90% as shown in Fig. 2, i.e., $\lambda_{\text{RF}} = 5 \times 10^{-4} \text{ m}^{-2}$ and $\lambda_{\text{THz}} = 4 \times 10^{-3} \text{ m}^{-2}$ in HRS protocol. As shown in Fig. 3, the coverage probability drops dramatically as the desired rate threshold y_{th} increases from 400 Mbps to 800 Mbps. Moreover, comparing the blue and purple curves reveals that raising the transmission power of RF relays only improves performance when the data rate is below 500 Mbps, but has essentially no effect when it surpasses 500 Mbps. In general, increasing the transmission power of THz relays has a greater impact on performance than raising that of RF relays, particularly when the data rate is high.

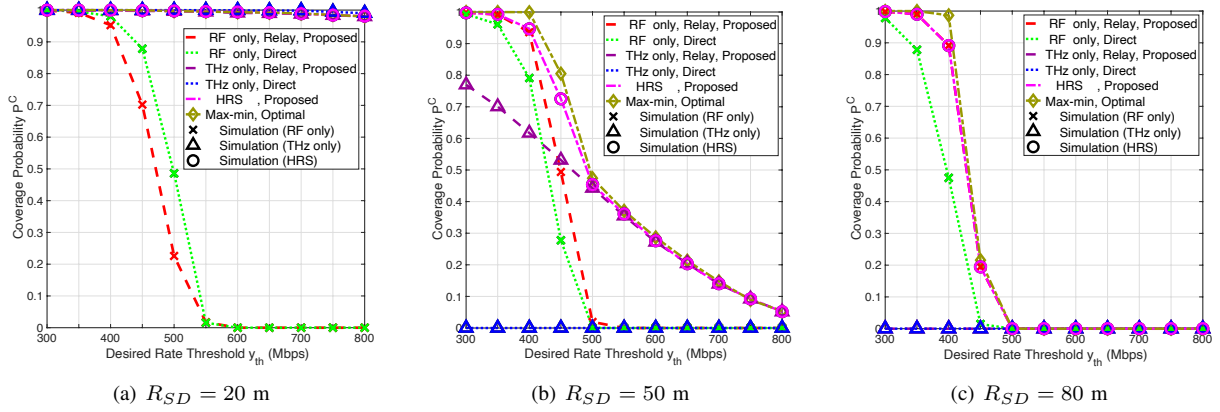


Fig. 5: Impact of different transmissions, the source-destination distance (R_{SD}), and desired data rate on coverage probability.

In Fig. 4, we set $\varepsilon_Q = 1$ W and select three sets of densities with 70% coverage as shown in Fig. 2, i.e., $\lambda_{RF} = \{0.45, 1.28, 2.27\} \times 10^{-4} \text{ m}^{-2}$, and $\lambda_{THz} = \{5, 3, 1\} \times 10^{-3} \text{ m}^{-2}$, respectively. As is shown in Fig. 4, the HRS coverage probability of THz relay dominated-network ($\lambda_{THz} = 5 \times 10^{-3} \text{ m}^{-2}$) is strongly influenced by the distance between source and destination R_{SD} , especially when $40\text{m} \leq R_{SD} \leq 60\text{m}$. The coverage probability of THz relay-dominated network decreases drastically as R_{SD} increases compared to RF relay-dominated network.

In Fig. 5, we compare the proposed HRS protocol with the optimal relay selection strategy according to the *max-min* selection scheme. We also compare the proposed protocol with RF-only relay selection and THz-only relay selection. For the sake of fairness, we compare the HRS protocol with RF and THz direct transmissions, which use the same channel model as the relay link. Notably, direct transmission takes only one time slot, whereas relay transmission requires two [15]. We set $\varepsilon_Q = 1$ W and the density of RF and THz relays are $\lambda_{RF} = 5 \times 10^{-4} \text{ m}^{-2}$ and $\lambda_{THz} = 4 \times 10^{-3} \text{ m}^{-2}$. We can notice in Fig. 5(a) that for short distances ($R_{SD} = 20$ m), RF relay selection and RF direct transmission have lower coverage probability and it starts decreasing drastically for higher data rates (500 Mbps), while $P^C \approx 1$ for other four transmission schemes. Hence, we conclude from Fig. 5(a) that for short distances: (1) it is better to use THz direct transmission when available than relay transmission; (2) the HRS protocol offers the same performance as the optimal protocol without requiring full and perfect CSI. In Fig.5(b), we can notice that for $R_{SD} = 50$ m, the THz direct transmission has zero coverage probability. We can also notice that for lower data rates (300 – 450 Mbps), RF relay and RF direct transmission offer better performance than THz relay. In contrast, for higher data rates (500 Mbps), the HRS protocol will select only THz relays since THz relay offers better performance since RF relay and RF direct transmission have a zero coverage probability. Finally, we notice that the proposed HRS protocol and the optimal protocol have nearly the same performance; and they both offer better performance than all the aforementioned schemes. In Fig.5(c), we can see that for large distances $R_{SD} = 80$ m, THz communications (direct and relay) have $P^C = 0$, and the HRS protocol will select only RF relays.

V. CONCLUSION

In this letter, the coverage probability expression of a proposed hybrid RF and THz relay selection protocol had been derived. The HRS protocol had mainly selected THz relays (associated with THz relays) for higher data rates or short source-destination distances, while it had mainly selected RF relays for lower data rates or large source-destination distances. The superiority of the HRS protocol had been demonstrated by comparing it with different strategies. In addition, the proposed HRS protocol had been compared with the optimal selection protocol, which requires a full and perfect instantaneous CSI of all the nodes in the networks. The HRS protocol had offered nearly the same performance as the optimal selection protocol for lower data rates, and the same performance for higher data rates.

REFERENCES

- [1] R. Wang, M. A. Kishk, and M.-S. Alouini, "Ultra-dense LEO satellite-based communication systems: A novel modeling technique," *IEEE Commun. Mag.*, vol. 60, no. 4, pp. 25–31, Apr. 2022.
- [2] H. Sariyeddeen *et al.*, "Next generation Terahertz communications: A rendezvous of sensing, imaging, and localization," *IEEE Commun. Mag.*, vol. 58, no. 5, pp. 69–75, May 2020.
- [3] T. S. Rappaport *et al.*, "Millimeter wave mobile communications for 5G cellular: It will work!" *IEEE Access*, vol. 1, pp. 335–349, May 2013.
- [4] G. Chattopadhyay *et al.*, "Compact Terahertz instruments for planetary missions," in *Proc. IEEE 9th Euro. Conf. on Antennas and Propagation*, Apr. 2015.
- [5] A.-A. A. Boulogeorgos and A. Alexiou, "Outage probability analysis of THz relaying systems," in *IEEE 31st Annu. Int. Symp. Personal, Indoor and Mobile Radio Commun.*, Oct. 2020, pp. 1–7.
- [6] S. Farrag *et al.*, "Outage probability analysis of UAV assisted mobile communications in THz channel," in *Proc. IEEE 16th Annu. Conf. Wireless On-Demand Netw. Syst. Services Conf.*, Mar. 2021, pp. 1–8.
- [7] S. Li and L. Yang, "Performance analysis of dual-hop THz transmission systems over $\alpha - \mu$ fading channels with pointing errors," *IEEE Internet Things J.*, pp. 1–1, Dec. 2021.
- [8] J. Sayehvand and H. Tabassum, "Interference and coverage analysis in coexisting RF and dense Terahertz wireless networks," *IEEE Wireless Commun. Lett.*, vol. 9, no. 10, pp. 1738–1742, Oct. 2020.
- [9] E. N. Pappasotiriou *et al.*, "An experimentally validated fading model for thz wireless systems," *Sci. Rep.*, vol. 11, no. 1, pp. 1–14, Sep. 2021.
- [10] H. Lei *et al.*, "Secrecy capacity analysis over $\alpha - \mu$ fading channels," *IEEE Commun. Lett.*, vol. 21, no. 6, pp. 1445–1448, Jun. 2017.
- [11] R. Wang, M. A. Kishk, and M.-S. Alouini, "Stochastic geometry-based low latency routing in massive LEO satellite networks," *IEEE Trans. Aerosp. Electron. Syst.*, vol. 58, no. 5, pp. 3881–3894, Aug. 2022.
- [12] M. Haenggi, *Stochastic Geometry for Wireless Networks*. Cambridge Univ. Press, 2012.
- [13] M. Alzenad and H. Yanikomeroglu, "Coverage and rate analysis for vertical heterogeneous networks (VHetNets)," *IEEE Trans. on Wireless Commun.*, vol. 18, no. 12, pp. 5643–5657, Dec. 2019.

- [14] I. Gordon *et al.*, “The HITRAN2016 molecular spectroscopic database,” *J. Quant. Spectrosc. Radiat. Transf.*, vol. 203, pp. 3–69, Dec. 2017.
- [15] K. Belbase, Z. Zhang, H. Jiang, and C. Tellambura, “Coverage analysis of millimeter wave decode-and-forward networks with best relay selection,” *IEEE Access*, vol. 6, pp. 22 670–22 683, 2018.